PHYSICAL REVIEW B VOLUME 46, NUMBER 7 15 AUGUST 1992-I

# Self-consistent Green's-function method for random overlayers

J. Kudrnovský
*Institute of Physics, Czechoslovak Academy of Sciences, CZ-180 40 Prague 8, Czechoslovakia*

I. Turek
*Institute of Physical Metallurgy, Czechoslovak Academy of Sciences, CZ-616 62 Brno, Czechoslovakia*

V. Drchal
*Institute of Physics, Czechoslovak Academy of Sciences, CZ-180 40 Prague 8, Czechoslovakia*

P. Weinberger
*Institute of Technical Electrochemistry, Technical University, A-1060 Wien, Austria*

N. E. Christensen
*Institute of Physics, Aarhus University, DK-8000 Aarhus C, Denmark*

S. K. Bose
*Department of Physics, Brock University, St. Catharines, Ontario, Canada L2S 3A1*
(Received 16 March 1992)

A tight-binding version of the linear-muffin-tin-orbital method is used to describe the electronic structure of random overlayers on a perfect substrate in a self-consistent manner within the local-density approximation. The true semi-infinite nature of the system is incorporated via the surface-Green's-function approach. A generalization of the coherent-potential-approximation method to treat inhomogeneous alloys is used to study the effect of disorder. The formalism is applied to evaluate the layer-projected densities of states and work functions of random Ag-Pd overlayers on a fcc Ag(001) substrate.

## I. INTRODUCTION

In this paper we report on the application of an efficient self-consistent Green's-function method for the calculation of electronic properties of random metallic surfaces. We consider in detail the case of a random overlayer on a nonrandom substrate. Such calculations are of vital importance in understanding how various physical properties of a clean surface change as a function of coverage by foreign atoms. The adsorption of transition metals on metallic substrates has been the subject of considerable experimental and theoretical investigations in recent years, since such studies contribute to the understanding of bimetallic catalysis, metal-metal interfaces, the properties of magnetic overlayers on nonmagnetic surfaces used in magnetic recording, etc. We aim at as realistic a description as possible and thus consider a true semi-infinite sample rather than its simulation via suitable slab or supercell. The study of electronic properties of surfaces, especially those covered by adsorbed atoms, must be carried out in a manner so that the potentials and the charge densities are consistent with each other. The lack of such self-consistency is the main source of uncertainties in empirical tight-binding (TB) calculations for overlayers and related systems. Finally, the study of surface states or work-function changes with coverage also requires a proper description of the vacuum-solid interface (the dipole barrier).

## II. FORMALISM AND THE THEORY

We have generalized our recent theory of the electronic structure of disordered overlayers[1] on metal substrates to include the charge self-consistency within the local-density approximation (LDA) and to treat the vacuum-solid interface properly. The main features of our method are (i) the application of the tight-binding linear-muffin-tin-orbital (TB LMTO) method[2] to describe the electronic structure from first principles; (ii) the description of the semi-infinite geometry of the system using the surface-Green's-function (SGF) formalism;[3] (iii) the use of the coherent-potential-approximation (CPA) approach extended to strongly inhomogeneous systems such as surfaces;[4] (iv) the characterization of the vacuum region by empty spheres which represent the continuation of the semi-infinite lattice to infinity;[5] and (v) the description of the Hartree and the exchange potentials within the spheres via the atomic-sphere approximation (ASA), while including both the monopole and the dipole terms of the charge density in the calculation of the Madelung potential.[6]

Due to the semi-infinite nature of the problem, all layers could, at least in principle, have different local physical properties. To make the problem tractable, we assume that from a certain layer onward, the electronic properties of all subsequent layers are those of the corresponding infinite system, namely, either a homogeneous

 

substrate or the vacuum. Thus, the semi-infinite sample is considered to be divided into three parts: (i) a homogeneous substrate with no disorder; (ii) a (homogeneous) vacuum represented by empty spheres with flat potentials; and (iii) an intermediate region consisting of several ($M$) atomic layers including a random overlayer, where all inhomogeneities (chemical, structural, or electric) of the system are concentrated and which also contains a few layers of empty spheres of the vacuum-sample interface.

The central quantity to be determined is the configurationally averaged auxiliary resolvent of the system,

$$\bar{g}(z)=\langle [P(z)-S]^{-1}\rangle=[\mathcal{P}(z)-S]^{-1} . \tag{1}$$

Here, $P(z)$ is a site-diagonal potential function matrix describing the scattering properties of all atoms. In an overlayer $A_cB_{1-c}$ it takes randomly either $P^A(z)$ or $P^B(z)$ at a given site $R$, while in the substrate it equals $P^s(z)$. Within the LDA and the CPA, the nonrandom configurationally averaged coherent-potential function matrix $\mathcal{P}(z)$ is also a site-diagonal quantity:

$$\mathcal{P}(z)=\begin{cases}\mathcal{P}_p(z)\\ p=1,2,\ldots,M \text{ in the intermediate region}\\ P^s(z) \text{ or } P^v(z) \text{ otherwise} ,\end{cases} \tag{2}$$

where the indices $s$ and $v$ refer to the substrate and vacuum regions, respectively, and $P^s(z)$ is determined using the self-consistent bulk TB LMTO method. For cubic lattices studied in this work, $P^s(z)$ is a diagonal matrix with respect to the orbital momentum index $L=(l,m)$. Due to lowering of the symmetry at the surface, $\mathcal{P}_p(z)$ is nondiagonal with respect to $L$ even for cubic lattices.

In Eq. (1) $S$ refers to the screened structure constants[7] within the most localized muffin-tin-orbital representation. The structure constants contain all necessary information about the geometry of the system, including the substrate lattice structure, adsorption geometry of the adatoms, etc. The use of screened structure constants has two important advantages: (i) the configurational averaging within the CPA can be performed without additional constraints,[8] as $S$ in nonrandom by definition and $P(z)$ is random, but site diagonal, and (ii) the short-range character of $S$ allows us to introduce the concept[3,9] or principal layers (PL), which greatly facilitates the theoretical treatment.

Within this concept, the semi-infinite sample is viewed to be composed of PL's defined in such a way that only the nearest-neighbor PL's are coupled by the structure constant $S$. Depending on the lattice structure and the face of the system, a PL consists of one or more atomic layers. For the sake of simplicity, in this paper we limit ourselves to the case when a PL is equivalent to one atomic layer [e.g., fcc (001) or bcc (110) surfaces within the first (second) nearest-neighbor terms in $S$ for fcc (bcc) lattices]. The generalizations to the case of PL's consisting of more than one atomic layer is also possible.[10] We can further simplify the problem by neglecting possible relaxations of top samples layers (outward or inward shifts with respect to ideal bulk interlayer distances). Then, by using bulk screened structure constants and employing the translational symmetry parallel to the sample face, one gets

$$\begin{aligned} S_{pp}(\mathbf{k}_\parallel)&=S_{00}(\mathbf{k}_\parallel) ,\\ S_{pq}(\mathbf{k}_\parallel)&=S_{01}(\mathbf{k}_\parallel)\delta_{p+1,q}+S_{10}(\mathbf{k}_\parallel)\delta_{p-1,q} ,\end{aligned} \tag{3}$$

where

$$S_{pq}(\mathbf{k}_\parallel)=\sum_{\mathbf{R}\in\{\mathbf{R}_{pq}\}}\exp\{i\mathbf{k}_\parallel\cdot\mathbf{R}\}S(\mathbf{R}) . \tag{4}$$

Here, $\mathbf{k}_\parallel$ is a vector from the surface Brillouin zone (SBZ), and the symbol $\{\mathbf{R}_{pq}\}$ denotes a set of vectors that connect one site in the $p$th layer with all sites in the $q$th layer. In Eqs. (3) and (4) we made use of the fact that the bulk structure constants $S$ depend only on a difference vector $\mathbf{R}=\mathbf{R}_p-\mathbf{R}_q$.

The coherent-potential function matrices $\mathcal{P}_p(z)$ in the intermediate region, $1\le p\le N$, are found from a set of coupled inhomogeneous LDA and CPA equations. The CPA equations, in matrix form, are given by

$$\begin{aligned} &\sum_{\alpha=A,B}c_p^\alpha t_p^\alpha(z)=0 ,\\ &t_p^\alpha(z)=[P^\alpha(z)-\mathcal{P}_p(z)]\{1+\phi_p(z)[P^\alpha(z)-\mathcal{P}_p(z)]\}^{-1} .\end{aligned} \tag{5}$$

Here, $c_p^\alpha$ are layer-dependent concentrations of atoms $\alpha=A,B$ in the overlayer, which, in general, can consist of several atomic layers. One of the atom types can be, eventually, identical to the substrate atoms. We shall limit ourselves here to the simplest case of an overlayer consisting of a single atomic layer, but a more general case is obvious. For a particular site $\mathbf{R}_p$ in a given layer $p$, $t_p^\alpha(z)$ and $\phi_p(z)$ are the on-site elements of the single-site $t$ matrix and of the averaged resolvent $\bar{g}(z)$, $\phi_p(z)=\bar{g}_{\mathbf{R}_p\mathbf{R}_p}(z)$, respectively. Note that even for nonrandom layers in the intermediate region both $\phi_p(z)$ and $\mathcal{P}_p(z)$ are layer dependent due to the LDA self-consistency (a special case is the surface of a pure crystal substrate). The quantity $\phi_p(z)$ enters also the expression for the layer- and atom-resolved density matrix $\rho_p^\alpha(r)$, which is the central quantity for the LDA part of the problem:

$$\rho_p^\alpha(\mathbf{r})=\sum_{L,L'}\int^{E_F}Z_{pL}^\alpha(\mathbf{r},E)D_{p,LL'}^\alpha(E)Z_{pL'}^\alpha(\mathbf{r},\mathbf{E})dE . \tag{6}$$

Here,

$$Z_{pL}^\alpha(\mathbf{r},E)=R_{pL}s(r,E)Y_l(\hat{\mathbf{r}}) , \quad \mathbf{r}=(r,\hat{\mathbf{r}})$$

is the partial wave normalized to unity within the atomic sphere of radius $s^\alpha$, and $E_F$ is the Fermi level of the bulk substrate. The layer-, atom-, and orbital-resolved density-of-states matrix is given by

$$D^{\alpha}_{p,LL'}(E)=-\frac{1}{\pi}\,\mathrm{Im}F^{\alpha}_{p,LL'}(E+i0)\ ,$$

$$F^{\alpha}_{p,LL'}(z)=[\dot{P}^{\alpha}_{L}(z)]^{1/2}\times(\phi_p(z)\{1+[P^{\alpha}(z)-\mathcal{P}_p(z)]\phi_p(z)\}^{-1})_{LL'}\times[\dot{P}^{\alpha}_{L'}(z)]^{1/2}\ , \tag{7}$$

where $\dot{P}^{\alpha}(z)$ stands for $dP^{\alpha}(z)/dz$. The quantity $F^{\alpha}_{p,LL'}(z)$ is the on-site element of the physical, conditionally averaged Green's function[4,8] expressed in terms of the averaged auxiliary Green's function $\phi_p(z)$ to be determined below [see Eqs. (10)–(12)]. The radial part $R^{\alpha}_{pL}(r,E)$ of the partial wave is obtained from the solution of the Schrödinger equation corresponding to the spherical LDA potential,

$$V^{\alpha}_{p}(r)=-\frac{2Z^{\alpha}}{r}+V^{\alpha,H}_{p}(\tilde{\rho}^{\alpha}_{p}(\mathbf{r}))+V^{\alpha,\mathrm{xc}}_{p}(\tilde{\rho}^{\alpha}_{p}(\mathbf{r}))+\sum_{L'}\sum_{q}M^{sL'}_{pq}\bar{Q}^{L'}_{q}\ , \tag{8}$$

where

$$\bar{Q}^{L}_{p}=\frac{\sqrt{4\pi}}{2l+1}\sum_{\alpha=A,B}c^{\alpha}_{p}\left[\int_{0}^{s^{\alpha}}Y_L(\hat{\mathbf{r}})\left[\frac{r}{s^{\alpha}}\right]^{l}\rho^{\alpha}_{p}(\mathbf{r})d\mathbf{r}-Z^{\alpha}\delta_{l,0}\right]\ . \tag{9}$$

The quantity $Z^{\alpha}$ in Eqs. (8) and (9) is the atomic number. The first three terms in Eq. (8) represent, respectively, the potential from the nuclei, and the Hartree and the exchange-correlation contributions, all resolved with respect to the atom and layer indices. The superscript tilde indicates that the spherically symmetric part of the density matrix $\rho^{\alpha}_{p}(r)$ is used, as is common in the ASA approach. The last term in Eq. (8) describes the electrostatic potential acting on electrons in the $p$th layer which results from the redistribution of electron density (as compared with the homogeneous substrate) among layers in the intermediate region due to the presence of the surface with adsorbed atoms. The resulting charge density is highly nonspherical at the surface and requires a proper treatment. As shown recently by Skriver and Rosengaard,[6] it is necessary to include not only monopole ($l=0$, $m=0$) but also the dipole ($l=1$, $m=0$, with the $z$ axis being normal to the surface) contributions to the multipole potential. The generalized intralayer and interlayer Madelung constants $M^{sL}_{pq}$ describe such interactions. The dipole potential barrier has thus contributions from net charges $\bar{Q}^{l=0}_{p}$ in atomic spheres (monopole terms) and those from the dipole charges $\bar{Q}^{l=1}_{p}$ in spheres. The latter ones are found from the corresponding nonspherical contributions to the density matrix, Eq. (6).

Two modifications, in the scheme used in Ref. 6, were introduced to evaluate the intersphere contribution to the electrostatic part of the potential. The first modification is due to the disorder and requires the statistical averaging of the multipole moments in each layer. The intersphere contributions, as well as the height $B_d$ of the electrostatic dipole barrier across the surface, are then evaluated as linear combinations of the layer-dependent averaged multipole moments [see Eq. (9)]. The second modification is due to the imperfect charge neutrality which is a direct consequence of the finite number of self-consistently treated layers. This problem was solved in Ref. 6 by an artificial shift of the potentials which restored the perfect charge neutrality. In contrast, we have left the charges in the surface region completely uncorrected but changed the reference points for an auxiliary electrostatic potential $\chi(\mathbf{r})$ produced by the multipole moments placed in the corresponding layers. The standard choice with the perfect charge neutrality is to set $\chi(\mathbf{r})$ to zero in the infinite depth in the bulk metal. The dipole barrier $B_d$ is then equal to the value of $\chi(\mathbf{r})$ at the infinite distance from the surface at the vacuum side. In our version, the reference point for the potential zero (dipole barrier) was taken in a lattice site of the first bulk (vacuum) layer not treated self-consistently. A detailed description of the corresponding Ewald technique will be given elsewhere. As in Ref. 6, we have restricted all multipole expansions to the monopole and dipole terms only.

An explicit expression for $\phi_p(z)$ is needed to solve both the CPA and the LDA equations. After performing a two-dimensional lattice Fourier transformation, one gets for the $(p,q)$ block $(1\le p,q\le N)$ of the inverse configurationally averaged resolvent $\bar{g}(\mathbf{k}_{\parallel},z)$,

$$\{\bar{g}(\mathbf{k}_{\parallel},z)\}^{-1}_{pq}=[\mathcal{P}_p(z)-S_{00}(\mathbf{k}_{\parallel})-\Gamma_p(\mathbf{k}_{\parallel},z)]\delta_{pq}-S_{01}(\mathbf{k}_{\parallel})\delta_{p+1,q}-S_{10}(\mathbf{k}_{\parallel})\delta_{p+1,q}\ , \tag{10}$$

where $\Gamma_p(\mathbf{k}_{\parallel},z)$ denotes the coupling of the intermediate region to the substrate (or vacuum), namely,

$$\Gamma_1(\mathbf{k}_{\parallel},z)=S_{10}(\mathbf{k}_{\parallel})\mathcal{G}^{v}(\mathbf{k}_{\parallel},z)S_{01}(\mathbf{k}_{\parallel})\ ,$$
$$\Gamma_p(\mathbf{k}_{\parallel},z)=0\quad\text{for } p=2,3,\ldots,M-1\ , \tag{11}$$
$$\Gamma_M(\mathbf{k}_{\parallel},z)=S_{01}(\mathbf{k}_{\parallel})\mathcal{G}^{s}(\mathbf{k}_{\parallel},z)S_{01}(\mathbf{k}_{\parallel})\ .$$

Note that the physical concept of the PL used in the method gives rise to the above matrix tridiagonal form of the Green's function $\bar{g}(\mathbf{k}_{\parallel},z)$ [Eqs. (10) and (11)]. The quantities $\mathcal{G}^{\lambda}(\mathbf{k}_{\parallel},z),\lambda=v,s$ are the SGF's of the vacuum and of the homogeneous sample substrate. By definition, the SGF is the top PL projection of the Green's function of the homogeneous semi-infinite substrate or vacuum,[3,9] and its knowledge is of central importance for the present formalism. The SGF's can be determined directly in real space by using the technique developed in Ref. 3, which avoids the use of the bulk resolvent common to other approaches[5,6,11] and reduces the problem to the following equations for $\mathcal{G}^{s}(\mathbf{k}_{\parallel},z)$ and $\mathbf{G}^{v}(\mathbf{k}_{\parallel},z)$:

$$\mathcal{G}^{s}(\mathbf{k}_{\parallel},z)=[P^{s}(z)-S_{00}(\mathbf{k}_{\parallel})-S_{01}(\mathbf{k}_{\parallel})\mathcal{G}^{s}(\mathbf{k}_{\parallel},z)S_{10}(\mathbf{k}_{\parallel})]^{-1}\ ,$$
$$\mathcal{G}^{v}(\mathbf{k}_{\parallel},z)=[P^{v}(z)-S_{00}(\mathbf{k}_{\parallel})-S_{10}(\mathbf{k}_{\parallel})\mathcal{G}^{v}(\mathbf{k}_{\parallel},z)S_{01}(\mathbf{k}_{\parallel})]^{-1}\ , \tag{12}$$

which has to be solved self-consistently for each $\mathbf{k}_{\parallel}$ and

energy $z$. These SGF's provide the necessary coupling to the intermediate region. In other words, using the concept of the SGF allows one to reduce the original problem of infinite order in the layer index to an effective problem of finite order $M$.

The desired quantity $\phi_p(z)$ is obtained by integrating over the SBZ of the $(p,p)$ block of $\bar{g}(\mathbf{k}_\parallel,z)$, namely,

$$\phi_p(z)=\frac{1}{N_\parallel}\sum_{\mathbf{k}_\parallel}\bar{g}_{pp}(\mathbf{k}_\parallel,z)\ . \tag{13}$$

In this equation, $N_\parallel$ is the number of atoms in a given layer. This completes the formal development of the theory.

## III. NUMERICAL RESULTS AND DISCUSSIONS

The theory is illustrated for the case of random $Ag_{1-c}Pd_c$ overlayer on the fcc (001) face of Ag substrate assuming an ideal epitaxial growth. This means that all interatomic distances in the overlayer, as well as between overlayer and substrate, are assumed to be the same (and equal to that in the Ag substrate). This is the case of the substrate-supported overlayer which frequently occurs in the experiment. Based on extensive tests, we have chosen the intermediate region consisting of three sample layers (an overlayer and two substrate layers), plus two layers of empty spheres simulating the vacuum. In this region the potentials are varied until the self-consistency with respect both to the LDA and the CPA is obtained. For exchange correlation we used the functional of Ceperley and Alder[12] as parametrized by Perdew and Zunger.[13] For $\mathbf{k}$-space integration we use 21 special $\mathbf{k}_\parallel$ points[14] in an irreducible ($\frac{1}{8}$th) part of the SBZ of the fcc (001) face.

The Fermi level of the system is that of the substrate bulk found from the condition

$$Z^s=-\frac{2}{\pi}\sum_L\int^{E_F}\dot{P}^s_L(E)\,\mathrm{Im}\phi^s_L(E+i0)dE\ , \tag{14}$$

where $Z^s$ is the number of the substrate valence electrons. The quantity $\phi^s_L(z)$ is usually determined by a different $\mathbf{k}$-space integration than that used for $\phi_p(z)$, Eq. (13), namely, we should integrate over the bulk fcc BZ,

$$\phi^s_L(z)=\frac{1}{N}\sum_k\{[P^s(z)-S(k)]^{-1}\}_{LL}\ . \tag{15}$$

Here, $N$ is the number of atoms in the sample. To avoid this ambiguity, we have determined $\phi^s(z)$ by integrating over the SBZ of the expression

$$\mathcal{G}^s(\mathbf{k}_\parallel,z)=[P^s(z)-S_{00}(\mathbf{k}_\parallel)-\Gamma^s_{00}(\mathbf{k}_\parallel,z)-\tilde{\Gamma}^s_{00}(\mathbf{k}_\parallel,z)]^{-1}\ . \tag{16}$$

Here, $\Gamma^2_{00}$ is the same as $\Gamma_M$, while $\tilde{\Gamma}^s_{00}$ is obtained from $\Gamma_1$ after substitution $P^v$ by $P^s$ [see Eqs. (11) and (12)]. The terms $\Gamma^s_{00}$ and $\tilde{\Gamma}^s_{00}$ couple the isolated layer of substrate atoms [the first two terms in Eq. (16)] to the semi-infinite substrate and its conjugate subspace, respectively. The result is the infinite crystal, and

$$\phi^s_L(z)=\frac{1}{N_\parallel}\sum_{\mathbf{k}_\parallel}\mathcal{G}^s_{LL}(\mathbf{k}_\parallel,z)\ . \tag{17}$$

Note that while in (15) the poles of resolvent are on the real axis, for $\mathcal{G}^s_{LL}(\mathbf{k}_\parallel,z)$ they are shifted to the complex plane making the $\mathbf{k}$-space integration numerically more convenient. The integration over the $\mathbf{k}_\perp$ component was already done implicitly[3] by evaluating corresponding SGF's.

In each iteration loop, one CPA and one LDA step is performed. We considered self-consistency to be achieved when the maximum differences among the input and output potentials in the intermediate region were below 0.01 Ry. This corresponds to at least a mRy accuracy in the calculated eigenvalues.

The charge neutrality in the intermediate region as a whole was preserved within an accuracy of $10^{-3}e$. Due to the finite height of the surface barrier, some charge is found outside the sample in the vacuum [typically $\approx(0.2-0.25)e$]. It gives rise to the lowering of the potential on the vacuum side of the sample-vacuum interface (imagelike potential). This result of self-consistent calculations with a proper description of the sample-vacuum interface indicates the limited validity of the "local neutrality concept" applied to each layer separately and frequently used in the empirical TB models.[15] On the second Ag substrate layer, i.e., the third sample layer, the number of electrons was close to 11 with an accuracy of $10^{-3}e$ in all cases. Also, the calculated dipole moments, which serve as a measure of the charge "nonsphericity," were essentially zero on the second substrate layer in all cases.

The results for the layer-resolved density of the states (DOS) are presented in Fig. 1 for the case of a clean Ag(001) surface and in Figs. 2, and 3 for a random $Ag_{75}Pd_{25}$ overlayer on Ag(001). In both cases we also present the results of non-self-consistent calculations, using, as an input, potentials from self-consistent calculations for bulk Ag and Pd. These calculations were performed using the same computer program but with the parameter controlling the mixing of the old and new potentials during the LDA loop set to zero. In the vacuum region, outside the sample, the potential in the two layers of empty spheres is chosen to rise in a staircase manner, with the height of the surface barrier adjusted to the experimental work function (4.64 eV). In the self-consistent calculation the potentials in these two layers are also determined self-consistently.

We mention the overall narrowing of the DOS in the surface layer of a clean Ag(001) surface (Fig. 1) compared to the bulk due to reduction of nearest neighbors from 12 in the bulk to 8 at the surface. The weight of the surface DOS is shifted towards higher energies as a result of self-consistency (resulting in a triangular shape characteristic of a surface DOS), the effect of which is missing in the non-self-consistent version. These findings are in accord with the results of self-consistent calculations using the slab method.[16,17] On the other hand, the results of empirical TB calculations,[15] which employ the heuristic concept of local orbital charge neutrality in each layer, overestimate the shift of the weight of the surface DOS

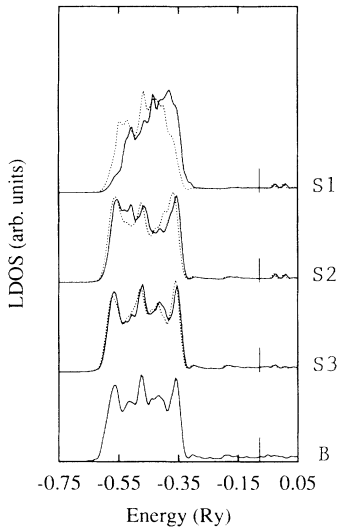


FIG. 1. Layer-resolved DOS's for a clean Ag(001) surface. The top three layers are denoted by $S1$, $S2$, and $S3$, respectively, while $B$ refers to the bulk layer. The vertical lines denote the position of the bulk substrate Fermi level. The self-consistent (solid lines) as well as non-self-consistent (dashed lines) DOS's are shown.

towards higher energies. We wish to point out the efficient damping of the surface-induced features into the bulk, which justifies, *a posteriori,* our choice of the intermediate region consisting of three sample layers plus two layers of empty spheres simulating the vacuum.

The presence of the Pd atoms in the surface (Figs. 2 and 3) manifests itself in a well-separated extra peak above the Ag $d$-band complex. This impurity peak is much better pronounced than in the corresponding $Ag_{75}Pd_{25}$ bulk[8] alloy case, partly due to the narrowing of the DOS at the surface (present in both self-consistent and non-self-consistent cases) but first of all due to the charge self-consistency effects. This effect is quite pronounced compared with the non-self-consistent case (Fig. 3), resulting in an appreciable shift of the Pd-$d$ states towards the substrate Fermi level and thus increasing the level difference between the $d$ states of Ag and Pd (an increase of the site-diagonal disorder). We note that while charge neutrality is preserved in the intermediate region as a whole, it does not apply to each layer in question. The adjustment of the alloy species levels is thus much more delicate than in the corresponding bulk alloy case and calls for a proper self-consistent treatment. The decomposition of the overlayer DOS into atom-resolved parts clearly shows that the peak above the Ag $d$-band complex is actually due to the Pd atoms. Only a very small Pd-induced feature survives in the corresponding energy region in the layer DOS beneath the surface.

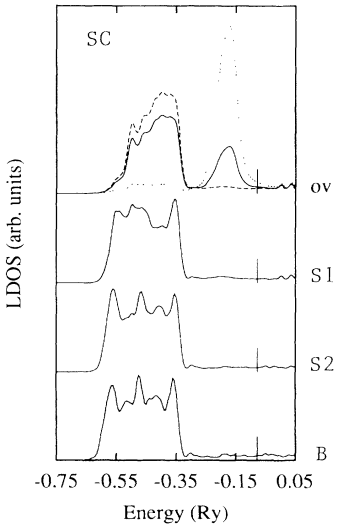


FIG. 2. Layer-resolved DOS's for an overlayer (ov) of random $Ag_{75}Pd_{25}$ on an Ag(001) surface calculated self-consistently (SC). The first two layers of the substrate are denoted by $S1$ and $S2$, while $B$ refers to the bulk layers. For the overlayer the componentlike DOS's for Ag (dashed line) and Pd (dotted line) are shown. The vertical lines denote the position of the substrate Fermi level.

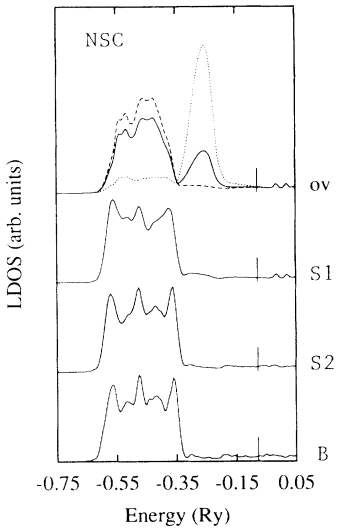


FIG. 3. The same as in Fig. 2, but for the non-self-consistent (NSC) case.

The work function (WF) was calculated using the expression $E_{WF}=B_d-E_F$, where $B_d$ denotes the electrostatic dipole barrier.[6] The $E_{WF}$'s of the $Ag_{1-c}Pd_c$ overlayer on the Ag(001) substrate are summarized in Table I. The value of 4.78 eV for the $E_{WF}$ of a clean Ag(001) surface agrees well with that obtained in Ref. 16 using the film linearized augmented plane wave (FLAPW) method for an 11-layer slab (4.74 eV). The value of 4.95 eV was found recently using the embedded SGF method,[18] while values of 4.2 eV were obtained in first self-consistent studies[17,19] for very thin slabs or using very small number of $\mathbf{k}_\parallel$ points. It is the dipole barrier which is sensitive to the number of $\mathbf{k}_\parallel$ points, while the electronic structure itself, for example, the DOS or the potential parameters, is less sensitive. The values ranging from 4.2 to 4.64 eV were found experimentally.[20] The recent measurements agreed on the value 4.4–4.45 eV. One possible explanation for the lower observed $E_{WF}$ compared with the calculated LDA value may be roughness of the surface.[16] We model

TABLE I. The calculated work functions for a clean Ag(001) surface and for a $Ag_{1-c}Pd_c$ random overlayer on a Ag(001) substrate.

| Clean Ag(001) | $Ag_{75}Pd_{25}$ on Ag(001) | $Ag_{50}Pd_{50}$ on Ag(001) | $Ag_{25}Pd_{75}$ on Ag(001) | Monolayer of Pd on Ag(001) |
|---|---|---|---|---|
| 4.78 eV | 5.03 eV | 5.25 eV | 5.45 eV | 5.67 eV |

the rough surface via a random overlayer of Ag atoms and vacancies on an otherwise perfect Ag substrate (a "sandpaper" model). The vacancies are represented by empty spheres with potentials determined self-consistently, as in the case of Pd atoms. The same formalism can be applied. For about 20% vacancies, the $E_{WF}$ was lowered from 4.78 down to 4.45 eV.

The $E_{WF}$ of a random (Ag, Pd) overlayer monotonically increases with the Pd content. To have a feeling for the calculated values, we have also determined the $E_{WF}$ of a clean fcc Pd(001) surface, both at the experimental lattice constant and for the expanded lattice (equal to the Ag lattice) corresponding to a supported Pd overlayer on the Ag(001) substrate. The calculated $E_{WF}$'s are, respectively, 5.83 and 5.61 eV. The former one agrees well with the experimental value of 5.8 eV in Ref. 20, while the latter one is in good agreement with value obtained for the Pd monolayer on the Ag(001) surface (see Table I).

We wish to demonstrate an essential importance of the proper determination of the surface dipole barrier for the $E_{WF}$ calculations. We have calculated the $E_{WF}$ of an Ag(001) surface without the contribution from the dipole charges [the $l=1$ term in Eqs. (8) and (9) omitted]. Alternatively, we have also performed the LMTO-ASA calculations for an 8 Ag+10 ES supercell [eight fcc (001) layers of Ag and ten layers of empty spheres (ES) separating them] and for a 9 Ag+9 ES supercell which also neglect the dipole charge contributions. In all three cases the calculated $E_{WF}$ was in the range of 7.1–7.2 eV. On the contrary, the layer DOS's and related quantities are rather insensitive to the exact value of the surface barrier. This justifies the use of simplified TB calculations using the infinite value of the surface barrier, for some specific surface-related problems.

We also present estimates of the surface core-level shifts (CLS) for clean Ag(001) and Pd(001) surfaces. The surface CLS is the energy difference between the surface- and bulk-atom core levels. One way[21] to obtain the surface CLS is to subtract the surface energies of atoms from the atomic number $Z$ and $Z+1$, e.g., for a Pd atom we thus need the surface energies of Pd and Ag surfaces. As our calculations do not use the frozen-core approximation and the same Hamiltonian and approximations are used for both the surface and the bulk, we estimate the surface CLS by subtracting the corresponding values of core-level energies (3$d$ for Ag or Pd). We are aware of the fact that core levels are strongly influenced by the many-body effects[22] due to the screening of the core hole created during the photoemission excitation, which are not accounted for within the LDA. However, as far as the difference is concerned, these corrections, though not exactly the same for the surface and the bulk, should cancel out approximately. A shift towards lower binding energies and the value of 0.44 eV for the surface CLS for Pd(001) were obtained in a recent experiment.[21] We have obtained shifts in the experimentally observed directions with the values of 0.44 and 0.55 eV for Ag(001) and Pd(001) surfaces, respectively. We have also estimated the surface CLS from the corresponding values of valence $d$-state levels, which we have identified with the potential parameters $C_d$ of the TB-LMTO theory.[2,7] The results were essentially the same, giving 0.43 and 0.55 eV for Ag and Pd, respectively. The agreement with the experiment is comparable to that when the surface CLS is obtained from the surface energies, at least for Pd.[21]

Finally, we briefly compare our approach with those existing in the literature and which treat the semi-infinite sample geometry. The present method can be considered as a generalization of the approach of Skriver and Rosengaard[6] (developed for clean surfaces) to the case of disordered surfaces and overlayers, including the case of an incomplete overlayer. For the case of clean surfaces, our method differs from that of Ref. 6 in the way the SGF is determined and the interlayer Madelung constants are calculated. The embedded GF method of Inglesfield and Benesh[23] also treats the semi-infinite sample in a self-consistent manner, but its generalization to the disordered case is difficult, if at all possible. The same comment applies to the method of Krüger and Pollmann,[11] developed to treat periodic semiconductor surfaces. The self-consistent surface GF method of Scheffler and coworkers[24] is able to treat a localized surface defect on a semi-infinite crystal self-consistently. In the region of the adparticle, no shape approximation to the potential or charge density is applied, but the substrate potentials are taken from the bulk rather than the surface calculations. Also, this method cannot be generalized to the cases of random coverage or disorder in the sample. The CPA and the layer Korringa-Kohn-Rostoker (LKKR-CPA) methods were combined[25] to treat self-consistently the interface between two metals with possible disorder present. Only the monopole-monopole Madelung terms were included, which is justified for the case of the metallic interface with rather smooth changes of potential or charge density but not for the case of the sample-vacuum interface (at least when the evaluation of the work function or the position of the surface states is concerned). The straightforward way of determining the SGF in our method as compared to the evaluation of the renormalized propagator[25] in the LKKR theory, based on the techniques taken from the theory of low-energy electron diffraction, is a great advantage of the present approach both numerically and conceptually. As already mentioned, this is due to the use of the screened structure constants provided by the TB-LMTO formalism. We have been informed[26] that the work to generalize the

IKKR CPA in order to treat disordered surfaces along the lines developed in the present paper is in progress.

## IV. SUMMARY AND CONCLUSIONS

In conclusion, we have developed an efficient self-consistent Green's-function technique to calculate properties of disordered metal surfaces. Our approach is based on the LDA within the first-principles TB-LMTO method. In this approach both intralayer and interlayer interactions are short ranged, which greatly facilitates the evaluation of the surface Green's function needed for a proper description of the semi-infinite nature of the problem. The potentials are treated in the ASA but for the charge density we include both monopole and dipole terms in the multipole expansion, which accounts for its nonspherical shape at the vacuum-sample interface and which yields a correct value of the electrostatic surface barrier. The effect of disorder is included via the CPA capable of describing, from a unified point of view, various situations occurring in experiments: clean surface, various stages of adsorption ranging from a low coverage limit to the case of adsorbed multilayers, as well as such complex systems as the surface of a disordered alloy with a possible segregation of one alloy component at the sample surface.[4] Although not discussed in detail, the method is also capable of treating high-Miller-index surfaces and of including effects due to the expansion or contraction of interlayer distances at the surface. The study of surfaces of heavy transition metals and their alloys requires the inclusion of the relativistic effects in the formalism. The effect of electron correlations on metallic surfaces,[27] not accounted for properly within the LDA, should also be included in the theory. Such studies will be subjects of forthcoming papers. In conjunction with the generalized perturbation method,[28] our approach can supply the effective cluster interactions[29] needed for surface phase diagram and surface segregation phenomena studies from first principles.

## ACKNOWLEDGMENTS

Financial support for this work was provided by the Czechoslovak Academy of Science (Project No. 11015), the Austrian Ministry of Science (Project No. GZ 45.123/1-II/A/4/91), and the Natural Sciences and Engineering Research Council of Canada.

[1]J. Kudrnovský, B. Wenzien, V. Drchal, and P. Weinberger, Phys. Rev. B **44**, 4068 (1991).
[2]O. K. Andersen and O. Jepsen, Phys. Rev. Lett. **53**, 2571 (1984).
[3]B. Wenzien, J. Kudrnovský, V. Drchal, and M. Šob, J. Phys. Condens. Matter **1**, 9893 (1989).
[4]J. Kudrnovský, V. Drchal, and P. Weinberger, Phys. Rev. B **44**, 6410 (1991).
[5]W. Lambrecht and O. K. Andersen, Surf. Sci. **178**, 256 (1986).
[6]H. L. Skriver and N. M. Rosengaard, Phys. Rev. B **43**, 9538 (1991).
[7]O. K. Andersen, O. Jepsen, and M. Šob, in *Electric Band Structure and Its Applications,* edited by M. Yussouff (Springer-Verlag, Heidelberg, 1987), p. 1.
[8]J. Kudrnovský and V. Drchal, Phys. Rev. B **41**, 7515 (1990).
[9]F. Garcia-Moliner and V. R. Velasco, Prog. Surf. Sci. **21**, 93 (1986).
[10]M. Šob and J. Kudrnovský, in *Defects in Materials,* edited by P. D. Bristowe, J. E. Epperson, J. E. Griffith, and Z. Liliental-Weber, MRS Symposia Proceedings No. 209 (Materials Research Society, Pittsburgh, 1991), pp. 177–182.
[11]P. Krüger and J. Pollmann, Phys. Rev. B **38**, 10 578 (1988).
[12]D. M. Ceperley and B. J. Alder, Phys. Rev. Lett. **45**, 566 (1980).
[13]J. Perdew and A. Zunger, Phys. Rev. B **23**, 5048 (1981).
[14]S. L. Cunningham, Phys. Rev. B **10**, 4988 (1974).
[15]G. Alan, Phys. Rev. B **44**, 13 641 (1991).
[16]H. Erschbaumer, A. J. Freeman, C. L. Fu, and R. Podlucky, Surf. Sci. **243**, 317 (1991), and references therein.
[17]J. R. Smith, F. J. Arlinghaus, and J. G. Gay, Phys. Rev. B **22**, 4757 (1980).
[18]G. C. Aers and J. E. Inglesfield, Surf. Sci. **217**, 367 (1989).
[19]D. R. Hamann, L. F. Mattheiss, and H. S. Greenside, Phys. Rev. B **24**, 6151 (1981).
[20]See N. V. Smith and C. T. Chen, Phys. Rev. B **40**, 7565 (1989), for a recent compilation of experimental work functions of the late transition metals and the noble metals.
[21]R. Nyholm, M. Ovarfold, J. N. Andersen, S. L. Sorensen, and C. Wigren, J. Phys. Condens. Matter **4**, 277 (1992).
[22]P. H. Citrin and G. K. Wertheim, Phys. Rev. B **27**, 3176 (1983).
[23]J. E. Inglesfield and G. A. Benesh, Phys. Rev. B **37**, 6682 (1988).
[24]M. Scheffler, C. Droste, A. Fleszar, M. Ma'ca, G. Wachutka, and G. Barzel, Physica B **172**, 143 (1991).
[25]J. M MacLaren, S. Crampin, D. D. Vvedensky, and J. B. Pendry, Phys. Rev. B **40**, 12 164 (1989); S. Crampin, R. Monnier, T. Schulthess, G. H. Schadler, and D. D. Vvedensky, *ibid.* **45**, 464 (1992).
[26]R. Monnier (private communication).
[27]H. Hasegawa, J. Phys. Condens. Matter **4**, 1047 (1992).
[28]F. Ducastelle and F. Gautier, J. Phys. F **6**, 2039 (1976); G. Tréglia, B. Legrand, and F. Ducastelle, Europhys. Lett. **7**, 575 (1988).
[29]V. Drchal, J. Kudrnovský, L. Udvardi, P. Weinberger, and A. Pasturel, Phys. Rev. B **45**, 14 328 (1992).